Compact Objects and Binaries in Dense Star Clusters
Proceedings IAU Symposium No. 398, 2026
H. M. Lee, J. Hong & R. Spurzem, eds.
doi:10.1017/S1743921325103736

A 15 Year Microlensing Survey in Omega Centauri

Zack Freeman

University of Utah
201 Presidents' Circle
Salt Lake City, UT 84112, USA
email: rzacktodd@gmail.com

Abstract. Omega Centauri (ω Cen) is the most massive globular cluster in the Galaxy, providing the ideal environment for a large number of potential stellar mass black holes to be initially formed, as well as being retained due to the large escape velocity and extended relaxation time. However, ω Cen has been the focus of a long debate over whether there is a sub-population of stellar mass black holes or an intermediate mass black hole. In this work, we use roughly 14 years of archival Hubble Space Telescope observations to search for potential microlensing events caused by stellar mass black holes. We create synthetic data from simulations of ω Cen, which allows us to optimize our regression model and provides an idea of what real microlensing event statistics will reflect. We also report our detection completeness of the regression model and detail ongoing candidate follow-up.

Keywords. Black holes, Stars, Globular Clusters, Gravitational Lensing

1. Introduction

Globular clusters (GCs) are expected to have hundreds to thousands of black holes (BHs) born during their formation, but our understanding of the present day populations and distribution of these BHs is limited. By uncovering the distribution of BHs in GCs, we can gain a better understanding of potential Laser Interferometer Gravitational-Wave Observatory (LIGO) sources and where they originate, as well as understand the impacts that natal kicks have on the retention of BHs in star clusters. By searching for microlensing signatures within Omega Centauri (ω Cen), we can discover potential BH candidates and begin to answer these open questions.

ω Cen is a prime candidate to learn more about the questions proposed above. It is the most massive GC in the Milky Way, with a mass of 3.55e6 $M_{\odot}$(Baumgardt & Hilker 2018). This large mass translates into a high number of BHs initially formed and a high retention fraction due to the increased escape velocity. Not only is ω Cen the most massive GC, but it has also been observed extensively by the *Hubble Space Telescope (HST)* in the past 20 years. This temporal coverage is well matched to the duration of microlensing events that we expect to observe (roughly 1 year timescales, see Zaris et al. (2020)).

Dynamical studies have shown the need for a dark mass at the center of ω Cen, but it has long been discussed whether this dark mass is an intermediate-mass black hole (IMBH) (Noyola et al. 2008; Noyola et al. 2010; Baumgardt 2017) or can be explained by other properties (Anderson & van der Marel 2010; van der Marel & Anderson 2010; Zocchi et al. 2017). Zocchi et al. (2019) and Baumgardt et al. (2019) showed that a centrally concentrated cluster of stellar mass black holes is able to explain the observed

© The Author(s), 2026. Published by Cambridge University Press on behalf of The International Astronomical Union. This is an Open Access article, distributed under the terms of the Creative Commons Attribution licence (https://creativecommons.org/licenses/by/4.0/), which permits unrestricted re-use, distribution and reproduction, provided the original article is properly cited.

https://doi.org/10.1017/S1743921325103736 Published online by Cambridge University Press

kinematics. Häberle et al. (2024) recently added to this debate with the discovery of multiple fast-moving stars in the innermost region of ω Cen, providing strong evidence for an IMBH, but this finding does not exclude a significant mass contribution from stellar mass black holes.

The expected lensing events are expected to be firmly in the microlensing regime, where we see an increase in apparent brightness, but with the lensing scale far below our telescope resolution. We use the ∼500 HST exposures to search for microlensing signatures in the lightcurves of source stars caused by potential black hole lenses.

In Section 2, we describe the regression model we use to fit microlensing events, as well as the synthetic data set we use to tune our model and determine our completeness. Then, in Section 3, we detail the methods that we use to find lightcurves with potential microlensing events. Finally, in Section 5, we conclude this work and describe ongoing efforts.

2. Synthetic Microlensing Lightcurves

We use the set of microlensing equations, as derived by Einstein (1936) and taken here from Schneider (2006), to create a regression model to help identify potential lensing events in the data and to create synthetic microlensing events.

Using star cluster simulations (see Prieto et al. 2025), we can determine the distribution of microlensing parameters to create realistic synthetic events. We can then sample the distributions and inject the synthetic microlensing events into the lightcurves of the real data. To prevent any potential real microlensing events leaking into the synthetic data, we bootstrap over the epochs of the observations; this preserves our observational cadence and σ_G values (a robust standard deviation estimate that is less impacted by outliers, defined as: $\sigma_G = 0.7413 * (q75 - q25)$, where $q75$ and $q25$ are the 75th and 25th quartiles, respectively). We created 40,000 synthetic lightcurves with injected synthetic microlensing events.

We are then able to use our regression model (using the Bayesian framework, *Maximum a Posteriori*, where we use the magnification distribution from simulations as a prior distribution) to fit our lightcurves. An example of a synthetic lightcurve with a synthetic microlensing event injected can be seen in Figure 1, with the regression model best fit plotted as the light blue line. We then are able to fit the set of 40,000 synthetic lightcurves, allowing us to estimate our completeness, which can be seen in Figure 2.

3. Searching for Microlensing Events

Although we can fit our synthetic lightcurves with the regression model described in Section 2, it is difficult to determine which fits are truly potential microlensing events. For example, a spurious bright outlier could cause a large magnification fit; based on the fit parameters, it may seem at first to be a potential lensing event that we would want to inspect, but upon further inspection, it would be realized as a false positive. Since we know the synthetic lightcurves have synthetic events, we expect any real event to have statistics similar to those of our synthetic events; therefore, we can use post-regression statistics calculated on our real and synthetic lightcurves to assist in the search.

We calculated 2D histograms from two statistics of our real and synthetic lightcurves, counting the number of each in every bin (n_{synth} and n_{real}), then for each bin we calculated the ratio $n_{synth}/(n_{synth} + n_{real})$. This serves as an ad hoc likelihood of a lensing event being found in a lightcurve, where bin values closer to 1 suggest that a real lightcurve closely resembles synthetic lightcurves. We show an example of this approach in Figure 3, where the first statistic is the reduced chi-square value of the model fit, $Red.\chi^2_{model}$, and the second statistic is the difference between the reduced chi-square

https://doi.org/10.1017/S1743921325103736 Published online by Cambridge University Press

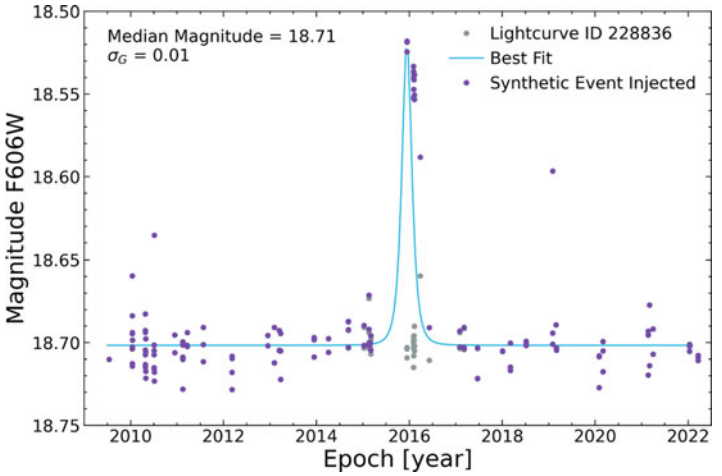


Figure 1. Lightcurve ID 228836 shown as the gray points. This lightcurve has a median magnitude = 18.71 and a $\sigma_G = 0.01$. The purple points show lightcurve ID 228836 with an injected synthetic lensing event. Injected values: max magnification = 1.2, epoch of max magnification = 2016, tranverse velocity = 16.8 km/s, distance between lens and source = 4 parsecs (pc). The blue line shows the best fit to the synthetic lightcurve.

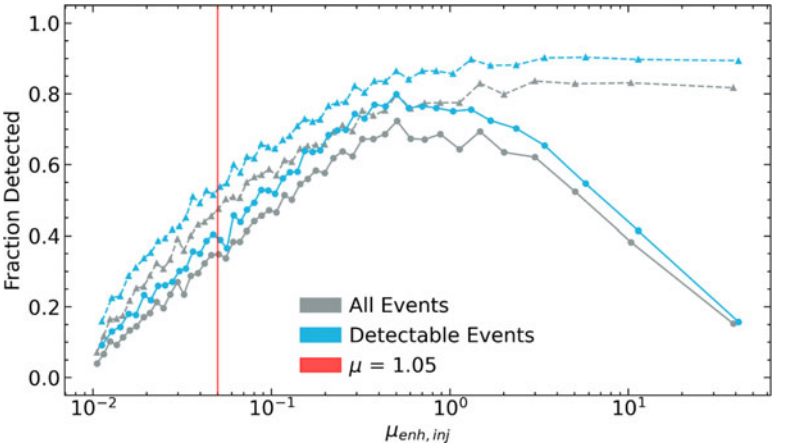


Figure 2. This figure shows the fraction of recovered events as a function of the enhanced injected magnification. The dashed lines with triangle markers represent events where the date was recovered, while the solid lines with circle markers represent where the date was recovered and was within 80% of the enhanced injected magnification. Each point contains 800 synthetic lightcurves; the enhanced injected magnification is the median value of the bin members.

value of a constant line, $Red.\chi^2_{constant}$ and $Red.\chi^2_{model}$. When this difference is large, the model has a statistically better fit than the constant line. For a given lightcurve, we can then determine what bin it falls within and the corresponding likelihood, and prioritize our search in this way.

4. Conclusion and Future Work

Candidate follow-up is currently ongoing with the approach detailed in Section 3, in addition to neural network approaches, where the post-regression statistics can be fed into a neural network which then outputs a likelihood of lensing. This allows for the use

https://doi.org/10.1017/S1743921325103736 Published online by Cambridge University Press

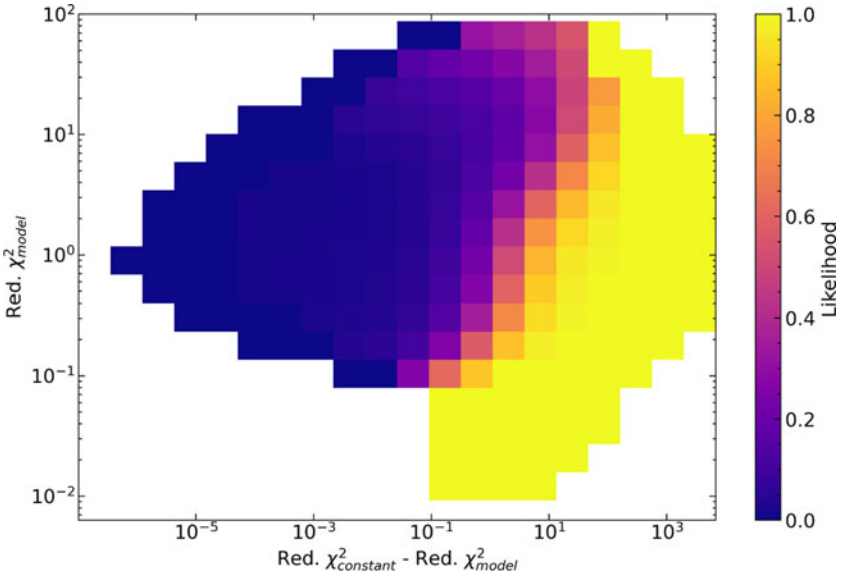


Figure 3. The difference in reduced chi squares between a constant line fit and the model line fit vs. the reduced chi square of the model line fit. Larger values along the x-axis indicate that the model line fit is statistically better than the constant line fit. The color bar represents an ad hoc likelihood, calculated by counting the number of lightcurves (synthetic and real) in each bin and using the equation $n_{synth}/(n_{synth} + n_{real})$. Real lightcurves in bins with lighter colors in the plot indicate a higher likelihood of a potential lensing event. A Gaussian kernel with a standard deviation of 1 has been applied to smooth the features.

of many different post-regression statistics to be used as input features and to model more complicated spaces, rather than the relatively small number of statistics that can be used with the 2D histogram approach.

Acknowledgments

Also contributing: Anil C. Seth, Maximilian Häberle, Andrea Bellini, Callie Clontz, Sebastian Kamann, Mattia Libralato, Nadine Neumayer, Carl Rodriguez, Jay Strader, Doga Veske, John Zaris. This project was funded in part by Hubble Space Telescope archival grant AR 17033.

References

Anderson, J., & van der Marel, R. P. 2010, ApJ, 710, 1032, doi: 10.1088/0004-637X/710/2/1032
Baumgardt, H. 2017, MNRAS, 464, 2174, doi: 10.1093/mnras/stw2488
Baumgardt, H., & Hilker, M. 2018, *MNRAS*, 478, 1520–1557, doi: 10.1093/mnras/sty1057
Baumgardt, H., He, C., Sweet, S. M., et al. 2019, *MNRAS*, 488, 5340–5351, doi: 10.1093/mnras/stz2060
Einstein, A. 1936, *Science*, 84, 506, doi: 10.1126/science.84.2188.506
Häberle, M., Neumayer, N., Seth, A., et al. 2024, arXiv e-prints, arXiv:2405.06015, doi: 10.48550/arXiv.2405.06015
Noyola, E., Gebhardt, K., & Bergmann, M. 2008, ApJ, 676, 1008, doi: 10.1086/529002
Noyola, E., Gebhardt, K., Kissler-Patig, M., et al. 2010, *ApJ*, 719, L60–L64, doi: 10.1088/2041-8205/719/1/l60
Prieto, E. G., Rodriguez, C. L., & Cabrera, T. 2025, Growing the Intermediate-mass Black Hole in Omega Centauri. https://arxiv.org/abs/2507.06316
Schneider, P. 2006, Extragalactic Astronomy and Cosmology

https://doi.org/10.1017/S1743921325103736 Published online by Cambridge University Press

van der Marel, R. P., & Anderson, J. 2010, ApJ, 710, 1063, doi: 10.1088/0004-637X/710/2/1063
Zaris, J., Veske, D., Samsing, J., et al. 2020, ApJ, 894, L9, doi: 10.3847/2041-8213/ab89a3
Zocchi, A., Gieles, M., & Hénault-Brunet, V. 2017, MNRAS, 468, 4429, doi: 10.1093/mnras/stx316
—. 2019, MNRAS, 482, 4713, doi: 10.1093/mnras/sty1508

https://doi.org/10.1017/S1743921325103736 Published online by Cambridge University Press